

## ESTIMATION OF MERCURY-SULFIDE SPECIATION IN SEDIMENT PORE WATERS USING OCTANOL–WATER PARTITIONING AND IMPLICATIONS FOR AVAILABILITY TO METHYLATING BACTERIA

JANINA M. BENOIT,\*†‡ ROBERT P. MASON,† and CYNTHIA C. GILMOUR‡

†The University of Maryland, Center for Environmental Studies, Chesapeake Biological Laboratory, P.O. Box 38, Solomons, Maryland 20688, USA

‡The Academy of Natural Sciences, Estuarine Research Center, 10545 Mackall Road, St. Leonard, Maryland 20685, USA

(Received 8 October 1998; Accepted 22 January 1999)

**Abstract**—The octanol–water partitioning of inorganic mercury decreased with increasing sulfide, supporting a model that predicts decreased fractions of neutral Hg-S species with increasing sulfide. These results help explain the decreased availability of Hg to methylating bacteria under sulfidic conditions, and the inverse relationship between sulfide and methylmercury observed in sediments.

**Keywords**—Mercury Methylmercury Partitioning Bioavailability Methylation

### INTRODUCTION

An inverse relationship between dissolved sulfide concentration and methylmercury (MeHg) production and/or concentration has been observed in sediments from a number of aquatic ecosystems [1–6]. Sulfide inhibition of Hg methylation may result from a decrease in the availability of substrate Hg to bacterial cells. However, this inhibition is not simply caused by decreased concentration of dissolved inorganic Hg ( $Hg_D$ ), due to precipitation of  $HgS_{(s)}$ , as is commonly speculated [2–4,7]. Filterable Hg concentrations do not decrease across sulfide gradients in natural sediments, but may increase [6,8]. Further, no correlation is found between  $Hg_D$  and MeHg in sediments [9]. An alternative explanation is that shifts in the complexation of  $Hg_D$  in pore waters may affect Hg bioavailability to bacteria. We have hypothesized that uptake of Hg by methylating bacteria is diffusive and that the observed sulfide inhibition can be explained by a decreasing fraction of neutral dissolved Hg complexes with increasing sulfide [6,9]. It has previously been shown that neutral chloride complexes of inorganic Hg are lipid soluble and that Hg uptake by phytoplankton [10,11] and Hg permeability across artificial membranes [12] both occur by passive diffusion.

The existence of a neutral Hg–monosulfide complex was proposed by Dyrssen and Wedborg [13,14], who estimated the concentration of  $HgS_{(aq)}^0$  that is in equilibrium with cinnabar through the reaction  $HgS_{(s)} = HgS_{(aq)}^0$ . The reaction constant (termed the intrinsic solubility) was extrapolated from the experimentally determined intrinsic solubilities of  $ZnS_{(s)}$  and  $CdS_{(s)}$  [14]. The existence of this complex and the magnitude of its formation constant remain conjectural, and several published models for cinnabar dissolution do not include  $HgS_{(aq)}^0$  [15–17]. Our own modeling efforts using formation constants gleaned from the literature, and including  $HgS_{(aq)}^0$ , suggest that at near neutral pH, the concentration of  $HgS_{(aq)}^0$  will decrease with increasing sulfide as it is replaced by disulfide complexes, primarily by  $HgHS_2^-$  [6]. This trend is consistent with observed

decreases in MeHg production in high-sulfide sediments if neutral species limit  $Hg_D$  availability to methylating bacteria.

One way to test the existence of neutral sulfide complexes is to measure partitioning from water into a hydrophobic solvent. In this investigation we report results of determinations of octanol–water partitioning ( $D_{ow}$ ) of  $Hg_D$  across a sulfide gradient. Because octanol–water partitioning depends on the hydrophobicity of Hg species, changes in  $D_{ow}$  across the gradient provide direct evidence for the existence of a neutral complex whose concentration depends on that of sulfide. Furthermore, because partitioning provides a surrogate for passive uptake [10,11], this study addresses a potential mechanism whereby sulfide may limit MeHg production and accumulation in natural sediments.

### MATERIALS AND METHODS

Partitioning experiments were carried out in 20-ml degassed 40 mM phosphate buffer containing 1 mg/L resazurin as a redox indicator. Buffer was adjusted to pH 6 for the first experiment and pH 7 for the second experiment using HCl or NaOH. Buffer aliquots were dispensed anaerobically into prepurged glass serum bottles. All labware was rigorously acid-leached and deionized-water rinsed, and trace-metal-clean laboratory protocols were used during the experiments. Teflon®-faced septa were applied to the serum bottles, and the head space was flushed with nitrogen. Titanium nitrilotriacetic acid reductant [18] was added via syringe to a concentration of 100  $\mu$ M. The standard redox potential of Ti(III) is –480 mV, and resazurin becomes colorless at an  $E_h$  of about –100 mV [19]. Buffer solutions turned from pink to clear upon addition of the titanium nitrilotriacetic acid, and only solutions that remained clear were used.

In the first experiment (pH 6), degassed Hg(II) standard in dilute  $HNO_3$  was added via syringe to each serum bottle to a final concentration of 500 pg/ml. The Hg was added after addition of sulfide. In the second experiment (pH 7), Hg(II) standard was added to the entire batch of buffer before dispensing in an effort to reduce the variability among replicates. In this experiment, sulfide was added after Hg. In both ex-

\* To whom correspondence may be addressed (benoit@acnatsci.org).

periments, solutions were shaken for 2 h before addition of octanol. Therefore, the equilibration period for Hg with sulfide was the same for both experiments.

Sulfide stock solutions were prepared in sealed, degassed bottles using degassed 40 mM phosphate buffer. All transfers were via syringe. Saturated  $\text{Na}_2\text{S}$  was diluted to produce a series of solutions ranging from 2 M to 0.2 mM. These were added to the buffer solutions to provide a sulfide gradient of 10 mM to 1  $\mu\text{M}$ . Each concentration was produced in quadruplicate for experiment 1 and in triplicate for experiment 2. Subsamples from two of each concentration were preserved in sulfide antioxidant buffer [20] and sulfide was measured using an Orion® (Beverly, MA, USA) silver-sulfide ion-specific electrode.

Octanol was deoxygenated by bubbling with  $\text{N}_2$  for several hours at room temperature. After a 2-h equilibration of the Hg- and sulfide-containing buffer solutions, 10- to 20-ml aliquots of degassed octanol were delivered into the serum bottles. Solutions were shaken for 2 h, then subsamples were taken from the water-only controls and the aqueous portion of the octanol-water mixtures and filtered through 0.2- $\mu\text{m}$  Acrodisc filters (Gelman Sciences, Ann Arbor, MI, USA) for Hg analysis. These subsamples were diluted, preserved with 1% HCl, and digested overnight with 0.5% BrCl before analysis for  $\text{Hg}_T$  using the cold-vapor atomic fluorescence spectrometry method of Gill and Fitzgerald [21] and Bloom and Fitzgerald [22]. The Hg concentration in the octanol was calculated by difference, taking into account the volumes of the two liquid phases. Aqueous pH was measured on separate aliquots.

Equilibrium speciation calculations were carried out using the MINEQL+ program (Environmental Research Software, Hallowell, ME, USA) to estimate the fraction of  $\text{Hg}_D$  present as a given complex. Because the experiments were performed at room temperature, the MINEQL+ simulations were run at 25°C. The formation constants chosen for Hg-S complexes that were used are given in the Appendix. These values represent average literature values rounded to the nearest 0.5 log units (see [6] for details). A value for the formation constant of  $\text{HgS}_{(\text{aq})}^0$  can be derived from the intrinsic solubility ( $K_{s1} = -10$ ) of cinnabar reported by Dyrssen and Wedborg [14] and the solubility product ( $K_{sp} = 36.7$ ) for cinnabar originally determined by Schwarzenbach and Widmer [17], to yield a rounded estimate for  $\log K_{s0}$  of 26.5 for the reaction  $\text{Hg}^{2+} + \text{HS}^- = \text{HgS}_{(\text{aq})}^0 + \text{H}^+$ . This value of  $K_{s0}$  provided good fit of a Hg speciation model to data from two disparate aquatic ecosystems [6]. All other equilibrium constants were from the MINEQL+ database.

## RESULTS AND DISCUSSION

Partitioning coefficients ( $D_{ow} = [\text{Hg}_{D-\text{octanol}}]/[\text{Hg}_{D-\text{water}}]$ ) for the two experiments are given in Table 1, along with the chemical equilibrium model-estimated percent of  $\text{Hg}_D$  present in neutral complexes. Increasing sulfide concentration decreased the hydrophobicity and partitioning of Hg into octanol. A decrease in octanol solubility is consistent with decreased passive uptake of Hg across hydrophobic cell membranes with increasing sulfide concentration. This decline in bioavailability provides a mechanistic explanation for the frequently observed inhibition of Hg methylation in sulfidic sediment pore waters.

Water-only controls from the experiments had an average  $\text{Hg}_D$  concentration lower than the calculated solubility of  $\text{HgS}_{(\text{s})}$  (i.e., <20 ng/L). These controls indicated that 96% of the

Table 1. Results of the octanol-water partitioning experiments

Sulfide concentration (log M)	pH	$D_{ow}^a$	% $\text{Hg}_D$ present as $\text{HgS}_{(\text{aq})}^0$	% $\text{Hg}_D$ present as $\text{Hg}(\text{HS})_2^0$
Experiment 1				
$-5.8 \pm 0.04$	6.2	$25 \pm 6.9$	92	0
$-5.2 \pm 0.08$	6.2	$14 \pm 2.5$	61	5
$-4.3 \pm 0.04$	6.2	$5.8 \pm 2.6$	14	11
$-3.2 \pm 0.01$	6.2	$1.5 \pm 0.65$	2	12
$-2.1 \pm 0.01$	7.0	$0.46 \pm 0.12$	0	2
Experiment 2				
$-6.0 \pm 0.03$	7.0	$24 \pm 5.8$	83	0
$-5.4 \pm 0.01$	7.0	$11 \pm 3.9$	33	1
$-4.2 \pm 0.01$	7.0	$2.3 \pm 1.8$	5	2
$-3.2 \pm 0.02$	7.0	$0.84 \pm 1.1$	0	2
$-1.8 \pm 0.02$	7.9	$-0.17 \pm 0.09$	0	0

<sup>a</sup> Determined octanol-water partitioning.

added Hg was sorbed to glassware, and that adsorption rather than precipitation of cinnabar controlled  $\text{Hg}_D$ . Adsorption was rapid, and it was complete within the 2-h equilibration period, before addition of octanol. Therefore, the concentration in the controls at the end of the experiment was assumed to represent the steady-state pool of dissolved Hg available for partitioning into the two phases.

Figure 1 shows the calculated speciation of mercury in the experimental solutions as a function of sulfide concentration. Together, sulfide complexes account for 100% of the  $\text{Hg}_D$  across the sulfide gradient. Two neutral dissolved Hg-S complexes are present in our model. Notice that the effect of increasing pH was to decrease the importance of  $\text{Hg}(\text{HS})_2^0$  relative to  $\text{HgS}_{(\text{aq})}^0$ . At the neutral and higher pH encountered in many

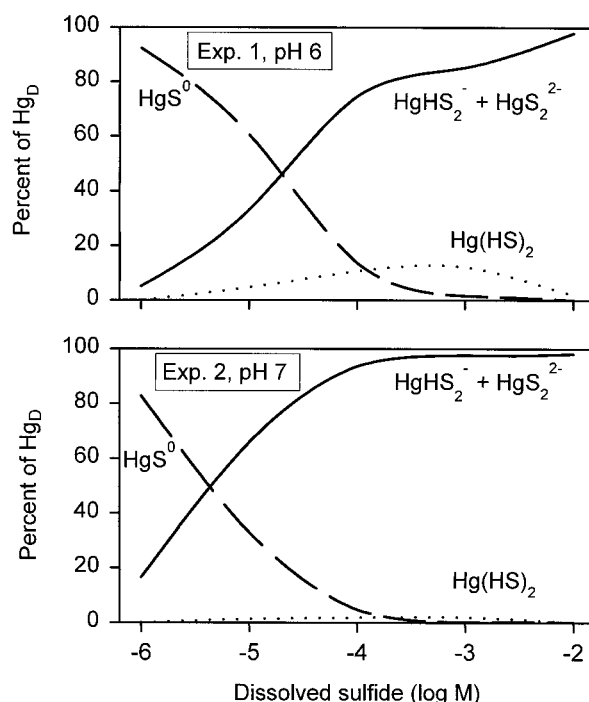


Fig. 1. Mercury speciation in the experimental solutions. The percent of total dissolved Hg ( $\text{Hg}_D$ ) present as various sulfide complexes is shown versus the sulfide gradient used in the experiments.

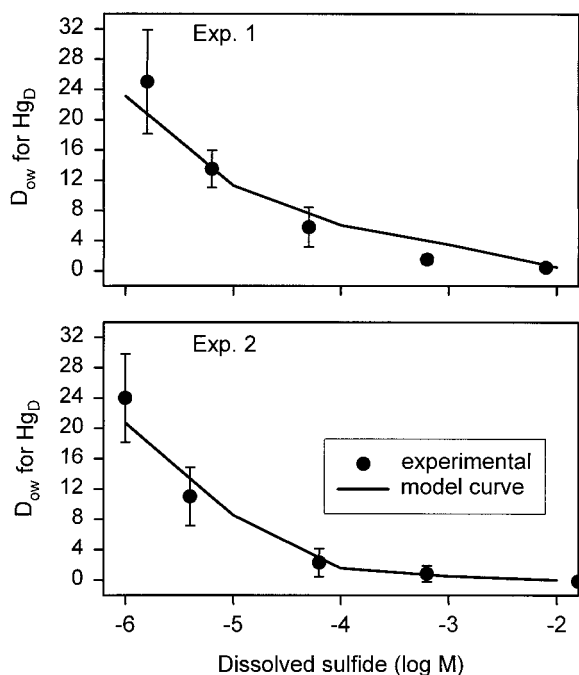


Fig. 2. Partitioning curves calculated with the chemical speciation model compared to measured octanol–water partitionings ( $D_{ow,s}$ ) from the two experiments. Model curves are shown for a value of  $K_{ow} = 25$  for neutral sulfide complexes ( $HgS_{(aq)}^0$  and  $Hg(HS)_2^0$ ).

aquatic sediments,  $HgS_{(aq)}^0$  dominates as the most important neutral Hg complex in the presence of excess sulfide.

In order to test the hypothesis that sulfide complexation decreased the partitioning of Hg by causing a shift in the speciation away from neutral  $HgS_{(aq)}^0$  toward charged complexes, we modeled  $D_{ow}$  for the experimental solutions using the relationship  $D_{ow} = \sum \alpha_i (K_{ow})_i$ , where  $K_{ow}$  is the partitioning coefficient of individual chemical species and  $\alpha$  is the fraction of Hg present as species  $i$  [after 11,12]. In experiment 1, all of the neutral dissolved Hg is present as  $HgS_{(aq)}^0$  at the lowest sulfide concentration and as  $Hg(HS)_2^0$  at the highest sulfide concentration (see Table 1), so  $K_{ow}$  for the two neutral complexes can be calculated using the endpoints of this experiment. Assuming that only neutral species partition significantly into octanol, at the high endpoint  $D_{ow} = 25 = 0.92(K_{ow})_{HgS_0}$  and at the low endpoint  $D_{ow} = 0.46 = 0.02(K_{ow})_{Hg(HS)_2}$ ; therefore  $K_{ow} = 27$  for  $HgS_{(aq)}^0$  and  $K_{ow} = 23$  for  $Hg(HS)_2^0$ . For simplicity, we used  $K_{ow} = 25$  for both complexes when calculating the expected  $D_{ow}$  for Hg across the sulfide gradients.

The model curves are compared to the experimentally determined  $D_{ow}$  distributions in Figure 2. The decline in  $D_{ow}$  across the sulfide gradient is consistent with the calculated decrease in the concentration of neutral sulfide species, which suggests that the observed change in partitioning across the sulfide gradient is driven by shifts in Hg–sulfide speciation. At low sulfide  $HgS_{(aq)}^0$  dominates, but disulfide complexes become more important as sulfide concentration increases. Near neutral pH, the major disulfide complex ( $HgHS_2^-$ ) is charged and hydrophilic, so partitioning of  $Hg_D$  is inhibited.

### CONCLUSIONS

The results demonstrate the existence of neutral dissolved Hg complexes in sulfidic solution. A chemical equilibrium

model including two neutral complexes successfully reproduced experimental  $D_{ow,s}$  for Hg. The model indicated that  $HgS_{(aq)}^0$  is the dominant dissolved neutral Hg complex determining lipid-solubility in sulfidic solutions at near neutral pH. The concentration of neutral dissolved Hg complexes decreases with increasing sulfide concentration, which is consistent with observed patterns of MeHg production and accumulation in aquatic ecosystems [5,6]. These results support our hypothesis that passive uptake of neutral dissolved Hg–S complexes may control the bioavailability of Hg to methylating bacteria. On the other hand, pore-water Hg complexation may depend on the presence of ligands other than sulfide, including dissolved organic carbon and polysulfides, in many natural sediments. Chemical equilibrium models of dissolved Hg complexation in pore waters may be useful in identifying ecosystems that are vulnerable to MeHg production and bioaccumulation.

**Acknowledgement**—This work was supported by the South Florida Water Management District (C-7690), the Florida Department of Environmental Protection (SP-434), and U.S. Geological Survey Cooperative Agreement Z929801. J. Benoit was supported by a Chesapeake Biological Laboratory Fellowship and a U.S. Environmental Protection Agency Star Fellowship.

### REFERENCES

- Craig PJ, Moreton PA. 1983. Total mercury, methyl mercury and sulphide in River Carron sediments. *Mar Pollut Bull* 14:408–411.
- Compeau G, Bartha R. 1983. Effects of sea-salt anions on the formation and stability of methyl mercury. *Bull Environ Contam Toxicol* 31:486–493.
- Compeau G, Bartha R. 1987. Effect of salinity on mercury-methylation activity of sulfate-reducing bacteria in estuarine sediments. *Appl Environ Microbiol* 53:261–265.
- Winfrey MR, Rudd JMW. 1990. Environmental factors affecting the formation of methylmercury in low pH lakes. *Environ Toxicol Chem* 9:853–869.
- Gilmour CC, Riedel GS, Ederington MC, Bell JT, Benoit JM, Gill GA, Stordal MC. 1998. Methylmercury concentrations and production rates across a trophic gradient in the northern Everglades. *Biogeochemistry* 80:327–345.
- Benoit JM, Gilmour CC, Mason RP. 1999. Sulfide controls on mercury speciation and bioavailability to methylating bacteria in sediments pore waters. *Environ Sci Technol* 33:951–957.
- Blum JE, Bartha R. 1980. Effect of salinity on methylation of mercury. *Bull Environ Contam Toxicol* 25:404–408.
- Bloom NS, Gill GA, Cappellino S, Dobbs McShea L, Driscoll R, Mason R, Rudd J. 1999. Speciation and cycling of mercury in Lavaca Bay, Texas sediments. *Environ Sci Technol* 33:7–13.
- Benoit JM, Gilmour CC, Mason RP, Riedel GF, Riedel GS. 1998. Behavior of mercury in the Patuxent River estuary. *Biogeochemistry* 80:249–265.
- Mason RP, Reinfelder JR, Morel FMM. 1996. Uptake, toxicity, and trophic transfer of mercury in a coastal diatom. *Environ Sci Technol* 30:1835–1845.
- Mason RP, Reinfelder JR, Morel FMM. 1995. Bioaccumulation of mercury and methylmercury. *Water Air Soil Pollut* 80:915–921.
- Gutknecht JJ. 1981. Inorganic mercury ( $Hg^{2+}$ ) transport through lipid bilayer membranes. *J Membr Biol* 61:61–66.
- Dyrssen D, Wedborg M. 1989. The state of dissolved trace sulphide in seawater. *Mar Chem* 26:289–293.
- Dyrssen D, Wedborg M. 1991. The sulphur–mercury (II) system in natural waters. *Water Air Soil Pollut* 56:507–519.
- Paquette K, Helz G. 1995. Solubility of cinnabar (red HgS) and implications for mercury speciation in sulfidic waters. *Water Air Soil Pollut* 80:1053–1056.
- Paquette K, Helz G. 1997. Inorganic speciation of mercury in sulfidic waters: The importance of zero-valent sulfur. *Environ Sci Technol* 31:2148–2153.
- Schwarzenbach G, Widmer M. 1963. Die Löslichkeit von Metallsulfiden. I. Schwarzes Quecksilbersulfid. *Helv Chim Acta* 46:2613–2628.

18. Moench TT, Zeikus JG. 1983. An improved method for a titanium(III) media reductant. *J Microbiol Methods* 1:199–202.
19. Gerhardt P. 1981. *Manual of Methods for General Bacteriology*. American Society for Microbiology, Washington, DC.
20. Brouwer H, Murphy TP. 1994. Diffusion method for the determination of acid-volatile sulfides (AVS) in sediments. *Environ Sci Technol* 13:1273–1275.
21. Gill GA, Fitzgerald WF. 1987. Picomolar mercury measurements in seawater and other materials using stannous chloride reduction and two-stage gold amalgamation with gas phase detection. *Mar Chem* 20:227–243.
22. Bloom N, Fitzgerald WF. 1988. Determination of volatile mercury species at the picogram level by low temperature gas chromatography with cold vapour atomic fluorescence detection. *Anal Chim Acta* 208:151–161.

## APPENDIX

Mercury-sulfide complexes and formation constants ( $K_f$ ) used in the chemical equilibrium model for dissolved Hg speciation

Reaction	Log $K_f$
$\text{Hg}^{2+} + \text{HS}^- = \text{HgS}_{(\text{aq})}^0 + \text{H}^+$	26.5
$\text{Hg}^{2+} + \text{HS}^- = \text{HgS}_{(\text{s})} + \text{H}^+$	36.5
$\text{Hg}^{2+} + \text{HS}^- = \text{HgSH}^+$	30.5
$\text{Hg}^{2+} + 2\text{HS}^- = \text{Hg}(\text{HS})_2^0$	37.5
$\text{Hg}^{2+} + 2\text{HS}^- = \text{HgS}_2\text{H}^- + \text{H}^+$	32.0
$\text{Hg}^{2+} + 2\text{HS}^- = \text{HgS}_2^{2-} + 2\text{H}^+$	23.5